Materials Science-Poland, 31(3), 2013, pp. 372-377
http://www.materialsscience.pwr.wroc.pl/
DOI: 10.2478/s13536-013-0116-6

VERSITA

Preparation of TiO_2/Al–MCM-41 mesoporous materials from coal-series kaolin and photodegradation of methyl orange

LI SHUIPING[1,2*], WU QISHENG[1], CUI CHONG[2], LU GUOSEN[3], ZHANG CHANGSEN[1], YAN ZHIYE[1]

[1]School of Materials Engineering, Yancheng Institute of Technology, Jiangsu Yancheng, 224051, P. R. China
[2]School of Materials Science and Engineering, Nanjing University of Science and Technology, Jiangsu Nanjing 210094, P. R. China
[3]College of Materials Science and Engineering, Nanjing University of Technology, Jiangsu Nanjing 210009, P. R. China

TiO_2/Al–MCM-41 mesoporous materials were prepared via sol-gel method by loading titania onto Al–MCM-41 mesoporous molecular sieve by hydrothermal treatment from coal-series kaolin as raw material. The TiO_2/Al–MCM-41 mesoporous materials were characterized by XRD, FT-IR, HRTEM, N_2 adsorption-desorption and the photocatalytic degradation of methyl orange solution under visible light irradiation. The results showed that the TiO_2/Al–MCM-41 mesoporous materials possessed a high surface area of 369.9 – 751.3 m^2/g and a homogeneous pore diameters of 2.3 – 2.8 nm. The titania crystalline phase was anatase, and the particles size of TiO_2 increased with TiO_2 content. The Al–MCM-41 mesoporous materials exhibited excellent photodegradation activity under visible-light irradiation for methyl orange.

Keywords: *coal-series kaolin; Al–MCM-41; TiO_2; photocatalytic degradation*

1. Introduction

Kaolin has a wide variety of applications in industry, particularly as ceramic material, adsorbent, and catalyst [1, 2]. Coal-series kaolin, as one kind of kaolin, has been investigated by researchers in many fields, such as zeolites, mesoporous materials, and intercalated materials [3, 4]. Nanoparticles of titania have a large specific surface area, which is responsible for the excellent performance [5, 6]. Because of its wide band gap of 3.0 – 3.2 eV, the effective industry applications of titania get bottlenecks. Since the discovery of mesoporous materials [7, 8], MCM-41 has attracted particular attention and was widely used as a catalyst and host for nanomaterials synthesis because of its high specific surface areas, uniform pore sizes and uniform and ordered mesoporous channels [9, 10]. In order to overcome the bottlenecks of commercials application of TiO_2 nanoparticles, there have been many work focused on the loading of TiO_2 nanoparticles onto MCM-41mesoporous materials [11, 12].

Wastewaters from various industries, factories, laboratories, etc. are serious problems to the environment [13]. Actually, in many cases, a lot of industrial wastewater streams are only slightly contaminated and contain low levels of dissolved organic compounds, such as dyes. In recent years, photocatalytic degradation of dyes using MCM-41 mesoporous materials loaded by TiO_2 nanoparticles or titanium has become very important [14, 15].

Our research group has devoted a lot of attention to the application of natural mineral materials and solid wastes, especially coal-measure kaolin. We synthesized basic molecular sieves [16], 4A zeolites [3], 5A zeolites [17] and mesoporous materials [4, 18]. Here, we report on the formation of TiO_2/Al–MCM-41 mesoporous materials using coal-measure kaolin as a starting material and the photocatalytic degradation of methyl orange by these mesoporous materials under visible light irradiation.

*E-mail: lishuiping2002@126.com

2. Experimental

2.1. Raw materials

The coal-series kaolin was supplied from the Xuzhou Coal Ming Group Corporation (China). The chemical composition of the coal-measure kaolin was determined by XRF (ARL Avant XP, Switzerland) and consisted of: SiO_2 39.24 %, Al_2O_3 36.12 %, CaO 0.39 %, TiO_2 0.65 %, K_2O 0.12 %, Na_2O 1.21 %, MgO 0.18 %, Fe_2O_3 0.89 %. Ignition loss was 20.78 %. Cetyltrimethylammonium bromide (CTAB), used as a template, was obtained from Shanghai Shanpu Chemical Co., Ltd. Sulfuric acid was supplied from Shanghai Shenxiang Chemical Reagent Co., Ltd. Sodium hydroxide was bought from Tianjin Bodi Chemical Co., Ltd. Tetrabutyl titanate was purchased from Tianjin Chemical Reagent No 1 Plant. Ethyl alcohol was obtained from Hangzhou Shuanglin Chemical Reagent Company. The above reagents were all analytical grade.

2.2. Synthesis of Al–MCM-41

Al–MCM-41 was synthesized through hydrothermal treatment as follows: CTAB and NaOH were dissolved in deionized water. The precursor prepared by selective leaching method from coal-series kaolin was then added into the mixed solution. The mixture was then transferred into a Teflon-lined steel autoclave and kept under hydrothermal condition at 110 °C with continuous stirring for 12 h. The resultant white product was filtered, washed for 3 times with deionized water, dried at 105 °C for 10 h, and calcined at 550 °C in air for 6 h to produce Al–MCM-41 mesoporous materials.

2.3. Synthesis of TiO_2/Al–MCM-41

TiO_2/Al–MCM-41 mesoporous materials were obtained from tetrabutyl titanate as Ti source in a typical synthesis. 1.0 g Al–MCM-41 was added into ethanol to form a solution, and then different amounts of tetrabutyl titanate were added to the solution and stirred for 45 min. A certain amount of distilled water was dropped into the above solution and stirred for 2 h. The white resultant product was washed and centrifuged with distilled water and ethanol for several times, dried at 80 °C for 8 h, and then calcined at 500 °C for 4 h to produce TiO_2/Al–MCM-41 mesoporous materials. The products were named as GS10, GS20, GS40, GS60 and GS80, where the Ti/Si mass ratio was 10, 20, 40, 60 and 80, respectively.

2.4. Characterization

The XRD data were collected by an Y500 full automatic diffractometer (Dandong, China) with Cu radiation at 30 kV and 20 mA (step size: 0.09° per step). A Fourier transform infrared spectrophotometer, NEXUS 670 (Nicolet, USA) with a spectral range from 4000 cm^{-1} to 400 cm^{-1}, was used to confirm the composition of the products. High-resolution transmission electron microscope, HRTEM (JEOL, JEM-2100, 200 kV) was used to characterize the size and the microstructure of the products. Nitrogen gas adsorption-desorption isotherms were measured at 77 K using a Coulter SA3100 (Beckman, USA).The specific surface area was calculated by the Brunauer-Emmet-Teller (BET) method ($P_s/P_0 = 0.05 - 0.20$). The total pore volume was obtained from the maximum amount of nitrogen gas adsorbed at a partial pressure $P_s/P_0 = 0.999$.

2.5. Activity measurements

The photocatalytic activity of TiO_2/Al–MCM-41 mesoporous materials was evaluated from the analysis of the photodegradation of methyl orange using a 300 W halogen lamp (a filter was used to cut-off the light with a wavelength bellow 400 nm). The UV-Vis spectra of methyl orange solution were detected every 30 min with a 722N UV-Vis spectrophotometer.

3. Results and discussion

Fig. 1 provides the X-ray diffraction patterns of Al–MCM-41 and TiO_2/Al–MCM-41 mesoporous materials. The diffraction pattern of Al–MCM-41 material has no distinctive diffraction peaks at 2θ ranging from 10 to 70°. On contrary, all TiO_2/Al–MCM-41 samples show anatase peaks. Moreover,

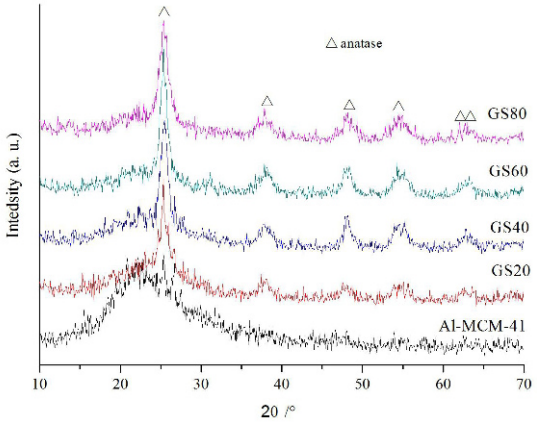

Fig. 1. XRD patterns of Al–MCM-41 mesoporous material and TiO_2/Al–MCM-41 mesoporous materials.

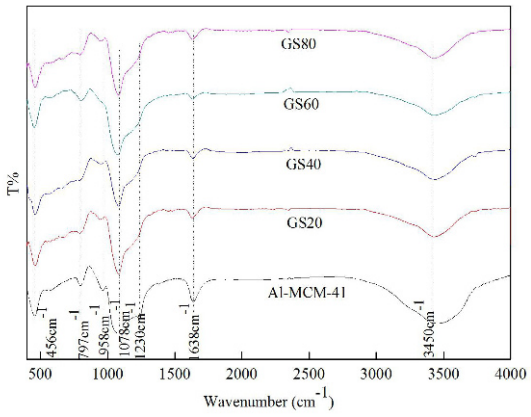

Fig. 2. FT-IR spectra of Al–MCM-41 and TiO_2/Al–MCM-41 mesoporous materials.

the intensity of all peaks for the TiO_2/Al–MCM-41, except GS80, increases with increasing TiO_2 content, which indicates that the addition of TiO_2 enhances the size of TiO_2 particles. The intensity decrease in the diffraction peaks of GS80 sample may be due to the crystalline transition of some amount of TiO_2 from anatase to amorphous phase. The TiO_2 particle diameter of anatase, calculated with Scherrer's equation using the line-width at half-maximum of the X-ray diffraction peaks at $2\theta = 26.1°$ was found to be in the range 8 – 19 nm for all the samples.

The FT-IR spectra of Al–MCM-41 and TiO_2/Al–MCM-41 are shown in Fig. 2. The vibration bands at 456, 797, 958 and 1230 cm^{-1} in Al–MCM-41 can be assigned to the bending vibrations of Si–O, vibrations of Al–O–Si, vibrations of Si–OH, vibrations of Si–O–H, respectively [19, 20]. The strong vibration band at 1078 cm^{-1}, which in Al–MCM-41 sample can be assigned to asymmetric stretching of Si–O–Si, has shifted to 1094 cm^{-1} in the spectra of TiO_2/Al–MCM-41 samples. Wave number for asymmetric stretching of Si–O–Si has shifted from lower to higher values when titanium was loaded onto Al–MCM-41. The strength of vibration bands at 797 and 1230 cm^{-1} in the spectra of Al–MCM-41 sample, which can be assigned to stretching of Al–O–Si and Si–O–H respectively [21], has decreased with increased titanium loading. In the spectra of our samples, the peak around 910 – 960 cm^{-1}, due to the Si–O stretching vibration of a polarized Si–O–Ti bond [22], has not been observed. But it is observed that the peak at 958 cm^{-1} in Al–MCM-41 sample, assigned to free vibration of Si–OH, is narrow and more intense as compared with the TiO_2/Al–MCM-41 samples. This may be due to the weak bond of Si–O–Ti [6].

High-resolution transmission electron microscopy (HRTEM) images of GS60 were collected to find out the location of TiO_2 (Fig. 3). As shown in Fig. 3a, a sheet structure of the mesoropous materials is observed, and the small dark spots representing TiO_2 have the particle size around 3 – 5 nm. The crystallite size of TiO_2 calculated from XRD is 8 – 19 nm, which is higher than that observed by HRTEM. This can be caused by the fact that the XRD patterns show only titania species of sufficient size [23]. For the TiO_2/Al–MCM-41 sample, no damage of the meroporous structure of the silicate framework is observed (as shown in Fig. 3b). It is concluded that the coating process and the thermal treatment probably have not destroyed the framework of Al–MCM-41 host. TiO_2 nanoparticles appear as dark substance among the channels on the surface of Al–MCM-41. In addition, a set of diffraction rings are observed in a selected area electron diffraction of TiO_2/Al–MCM-41 sample, which are indexed as the anatase phase of TiO_2, which is consistent with the XRD results.

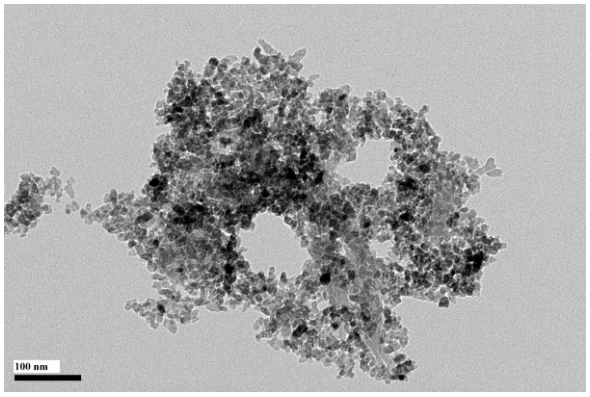

(a)

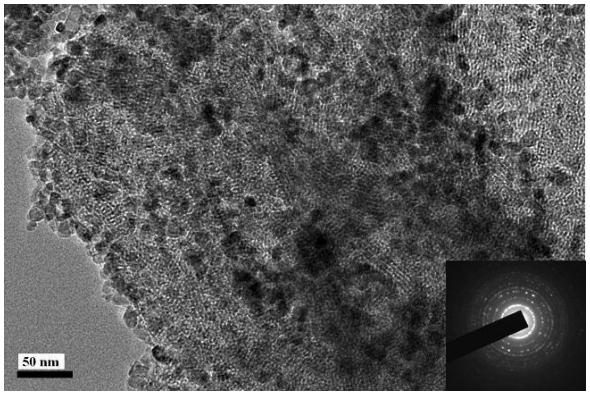

(b)

Fig. 3. HRTEM micrographs of sample GS60.

The adsorption-desorption isotherms of nitrogen at 77 K for the samples are shown in Fig. 4. The isotherms of all samples can be classified as the type IV, which according to the IUPAC convention is a typical isotherm of mesoporous material. For all the samples, the steep increase in N_2 gas adsorption is observed in the range of P_s/P_0 from 0.2 – 0.4 for Al–MCM-41 and GS20 samples and can be attributed to the presence of mesopores of a uniform size. In the range of $0.4 \leqslant P_s/P_0 \leqslant 0.9$, only slight increase in N_2 adsorption occurs. The increase of adsorption in the vicinity of $P_s/P_0 = 1$ corresponds to macropores formed by agglomeration of the mesoporous particles. The hysteresis loops in the isotherms are of H4 type. Little hysteresis in the whole range of the adsorption and desorption isotherms suggests that the mesopores in the sample are cylindrical, straight and uniform in size without a distinct throat. The rate of nitrogen adsorption was found to decrease with an increase in TiO_2 content. This reflected that the decrease in specific surface area, total pore volume and average pore size with an increase in TiO_2 coating as shown in Table 1.

Table 1. Structure of the samples derived from nitrogen sorption and HRTEM studies.

Sample	BET specific surface area (m^2/g)#	Total pore volume (ml/g)#	Average pore diameter (nm)
Al–MCM-41	1070	1.13	3.8#
GS20	751.3	0.63	2.8*
GS40	548.3	0.48	2.5*
GS60	372.3	0.39	2.5*
GS80	369.9	0.38	2.3*

Determined from nitrogen isotherm
* Determined from HRTEM images

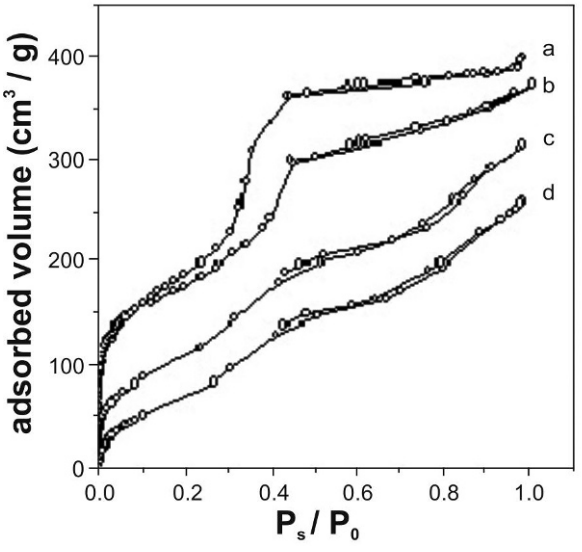

Fig. 4. Nitrogen adsorption-desorption isotherms for (a) Al–MCM-41, (b) GS20; (c) GS60 and (d) GS80.

The photocatalytic degradation curves of methyl orange under visible-light irradiation are displayed in Fig. 5. After the Al–MCM-41 mesoporous material had been dispersed into the methyl orange solution, a decrease in the concentration of methyl orange solution occurred, which was attributed to the adsorption of methyl

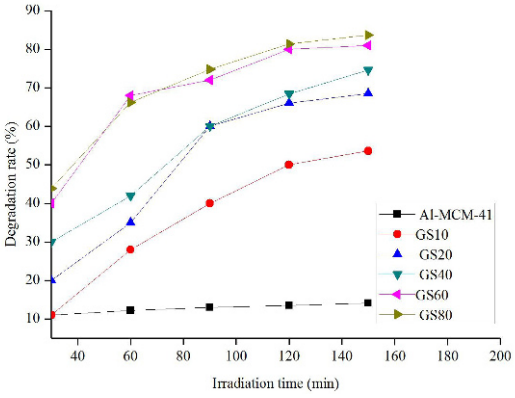

Fig. 5. Photocatalytic degradation curves of methyl orange.

orange molecules on the mesoporous material. It can be seen that the photocatalytic degradation rate increases with TiO_2 content and visible light irradiation time. These results indicate that TiO_2/Al–MCM-41 mesoporous materials from coal-series kaolin exhibit excellent visible-light photodegradation of methyl orange, which increases with increasing TiO_2 coating content. However, the photocatalytic degradation rates of methyl orange under visible-light irradiation are lower than the results of some reports [24–26], where the catalyst, loaded on mesoporous TiO_2, TiO_2 coated with anatase or TiO_2 modified with other ions, was irradiated under ultraviolet light.

4. Conclusions

TiO_2/Al–MCM-41 mesoporous materials with different ratios of TiO_2, using coal-series kaolin as a starting material were prepared at room temperature in ethanol solution by general sol-gel method. The photocatalysis properties of these mesoporous materials were also studied by photocatalytic degradation of methyl orange under visible light irradiation. The results showed that the TiO_2/Al–MCM-41 possessed a high surface area of 369.9 – 751.3 m^2/g and homogeneous pore diameters of 2.3 – 2.8 nm. TiO_2 nanoparticles entered the pore channel of Al–MCM-41 mesoporous materials and enhanced the photocatalytic properties of these materials. The TiO_2/Al–MCM-41 mesoporous material exhibited excellent visible-light activities for photodegradation of methyl orange, which increased with increasing TiO_2 coating content.

Acknowledgements

This work was supported by the Research Fund for Social Development Plan of the Science and Technology Department of Jiangsu provincial government (BS2007038), the National Natural Science Foundation of China (NSFC-51202211), and Academic Scientific Research Industrialization Projects of Jiangsu province (JHB2011-53), and Research fund of Key Laboratory for Advanced Technology in Environmental Protection of Jiangsu Province (AE201111).

References

[1] MA H. Z., WANG B., WANG Y., *J. Hazard. Mater.*, 145 (2007), 417.
[2] TOYA T., KAMESHIMA Y., NAKAJIMA A., OKAD K., *Ceram. Int.*, 32 (2006), 789.
[3] WU Q. S., LI S. P., SU S. S., *Chemical Industry Engineering and Progress*, 28 (2009), 130 (in Chinese).
[4] WU Q. S., LI S. P., SU S. S., *Chemical Industry Engineering and Progress*, 28 (2009), 458 (in Chinese).
[5] TUEL A., HUBERT-PTALZGRAT L. G., *J. Catal.*, 217 (2003), 343.
[6] LIHITKAR N. B., ABYANEH M. K., SAMUEL V., PASRICHA R., GOSAVI S. W., KULKARNI, S. K., *J. Colloid Interface Sci.*, 314 (2007), 310.
[7] KRESGE C. T., LEONOWICZ M. E., ROTH W. J., VARTULI J. C., BECK J. S., *Nature*, 359 (1992), 710.
[8] BECK J. S. et al., *Am. Chem. Soc.*, 114 (1992), 10834.
[9] WANG L. J., LI D., WANG R., HE Y., QI Q., ZHANG T., *Sens. Actuators, B: Chem*, 133 (2008), 622.
[10] CHEN H. Y., XI H. X., CAI X. Y., YU Q., *Microporous Mesoporous Mater.*, 118 (2009), 396.
[11] YANG H. M., DENG Y. H., DU C. F., *Colloids Surf., A*, 339 (2009), 111.
[12] SADJADI M. FARHADYAR S., N., ZARE K., *Superlattices Microstruct.*, 46 (2009), 77.
[13] AKPAN U. G., HAMEED B. H., *J. Hazard. Mater.*, 170 (2009), 520.
[14] XIE Y., LI Y. Z., ZHAO X. J., *J. Mol. Catal. A: Chem*, 277 (2007), 119.
[15] XIAO Y., DANG L. Q., AN L. Z., BAI S. Y., LEI Z. B., 29 (2008), 31.
[16] LI S. P., WU Q. S., *J. Mater. Sci. Eng.*, 27 (2009), 233 (in Chinese).
[17] LI S. P., WU Q. S., *Chin. Environ. Eng.*, 28 (2010), 403 (in Chinese).
[18] WU Q. S., LI S. P., *J. Wuhan University Tech. (Mater Sci. Ed.)*, 26 (2009), 514.
[19] MOENKE H. H. W.. Silica, the three dimensional silicates, borosilicates and beryllium silicates. The Infrared Spectra of Minerals, Mineralogical Society. London, 1974.

[20] KUBICKI J. D., BLAKE G. A., APITZ S. E., *Am. Mineral.*, 81 (1996), 789.
[21] KIYOSHI O., AKIRA S., TAKAHIRO T., SHIGEO H., ATSUO Y., KENNETH J. D. M., *Microporous Mesoporous Mater.*, 21 (1998), 289.
[22] XU H. L. et al., *J. Phys. Chem. Solids*, 72 (2010), 24.
[23] HSIEN Y.H., CHANG C. F., CHEN Y. H., CHENG S., *Appl. Catal. B*, 31 (2001), 241.
[24] YUAN S., SHENG Q. R., ZHANG J. L., *Microporous Mesoporous Mater.*, 110 (2008), 501.
[25] FAN X. X. et al., *J. Mol. Catal. A: Chem.*, 284 (2008), 155.
[26] HUANG J. H. et al., *Microporous Mesoporous Mater.*, 110 (2008), 543.

Received 2012-03-08
Accepted 2013-04-23